catalysts

MDPI

Article

The Nature of Active Sites in the Pd/C-Catalyzed Hydrogenation/Hydrodeoxygenation of Benzaldehyde

Sofia Capelli [1], Stefano Cattaneo [1], Marta Stucchi [1], Bart D. Vandegehuchte [2], Alessandro Chieregato [3], Alberto Villa [1] and Laura Prati [1,*]

[1] Dipartimento di Chimica, Università degli Studi di Milano, Via C.Golgi 19, 20133 Milano, Italy; sofia.capelli@unimi.it (S.C.); stefano.cattaneo2@unimi.it (S.C.); marta.stucchi@unimi.it (M.S.); alberto.villa@unimi.it (A.V.)
[2] TotalEnergies One Tech Belgium, Zone Industrielle Feluy C, B-7181 Seneffe, Belgium; bart.vandegehuchte@totalenergies.com
[3] TotalEnergies Research Center—Qatar (TRCQ), Qatar Science & Technology Park, Al Gharrafa, Doha P.O. Box 9803, Qatar; alessandro.chieregato@totalenergies.com
* Correspondence: laura.prati@unimi.it

Abstract: Hydrogenations and hydrodeoxygenations represent two of the most important reactions in the production of both bulk and fine chemicals. Despite the wide and long use of metal-based catalysts for this reaction, there is still some uncertainty with respect to the properties governing the catalyst activity. Using the hydrogenation of benzaldehyde as a model reaction, in this paper, we disclose the dominant parameters determining catalyst activity of Pd nanoparticles supported on a carbonaceous material (carbon nanoplates, GNP). In particular, several operating parameters of the catalyst synthesis were varied in order to obtain materials with differences in such physico-chemical properties as nanoparticle size, Pd oxidation state and Pd surface exposure. A linear correlation between catalyst activity and the amount of surface Pd(0) atoms was found; this dependence, maintained after catalyst recycling, pointed out the nature of the active site of the Pd/GNP catalyst represented by exposed Pd(0) species.

Keywords: catalytic active site; hydrogenation reaction; Pd/C catalyst

Citation: Capelli, S.; Cattaneo, S.; Stucchi, M.; Vandegehuchte, B.D.; Chieregato, A.; Villa, A.; Prati, L. The Nature of Active Sites in the Pd/C-Catalyzed Hydrogenation/Hydrodeoxygenation of Benzaldehyde. *Catalysts* **2022**, *12*, 251. https://doi.org/10.3390/catal12030251

Academic Editors: Adam F. Lee, Christopher Parlett, Sébastien Royer, Emma C. Lovell and Vladimir Sobolev

Received: 9 January 2022
Accepted: 17 February 2022
Published: 22 February 2022

1. Introduction

The ultimate goal in heterogeneous catalysis is the accurate design of a catalyst that drives the reaction to the desired products. In this sense, researchers are deeply studying the properties of catalysts to reach correlations between the activity of a catalyst and its features [1]. Moreover, thanks to the development of advanced characterization techniques, it is now possible to carefully study the physico-chemical properties of catalysts, making it possible to identify the discriminating factors for an active and selective catalyst.

It is well known that supported noble metal nanoparticles (NPs) are active in reduction reactions, although high temperatures and hydrogen pressures are often required [2,3]. The synthetic procedure of catalysts is a key factor that influences catalyst morphology. Supported metal NPs can be prepared by means of impregnation, deposition-precipitation, polyol processes, sol-immobilization and other techniques. Among these, sol-immobilization [4] is widely used since it makes it possible to obtain a narrow particle size distribution and a good metal dispersion regardless of the support [5–7]. The key feature of preparation by sol-immobilization is the use of capping agents [8–11], which prevent the agglomeration of NPs during both the their synthesis and immobilization steps, thus providing good metal dispersion on the support. However, the capping agent itself can also influence the final performance of metal NPs. On one hand, the presence of a stabilizer can decrease catalytic activity by hindering the access of the substrate to the active site [12]. On the other hand, recent studies revealed that capping agents increase

the complexity of the system by transferring charges at the organic-metal interface or by creating noncovalent interactions between the substrate and the ligand itself [13]. Therefore, capping agents not only impact the size of NPs [14,15], but they can also act as promoters by modifying the selectivity in various liquid-phase reactions [7,13]. From a catalytic point of view, many studies showed that the Pd NPs' sizes can largely influence the catalyst activity during the reduction of nitro compounds [16,17], the electrocatalytic reduction of CO_2 [18] and the hydrogenation of allyl alcohol [19], but some studies also highlighted the importance of the initial oxidation state of the active metal. Zorn et al. studied the influence of the oxidation state of Pd NPs within CO oxidation [20]. The authors found that alumina-supported Pd^0 NPs and sub-stoichiometric $PdO_x < 1$ NPs exhibited similar and high activities, while the full oxidized catalyst showed low activity. Similar results were obtained by Xiong et al. during hydrocarbon oxidation [21]. Qing et al. studied the role of Pd^0 and Pd^{2+} in the decomposition reaction of formic acid [22]. The authors found that metal Pd is the active species while PdO eliminates the undesired dehydration route, thus preserving the catalyst's selectivity. Furthermore, the effect of the Pd particle size and oxidation state on the activity and selectivity during muconic acid hydrogenation was evaluated [23], and it was shown that the increasing of Pd^0 contents improves the catalyst activity towards adipic acid formation.

In this work, Pd NPs supported on graphene nano-plates (GNP), a stable graphitic support, were synthesized by sol-immobilization. We chose a carbon support in order to limit strong metal-support interaction (SMSI) and, thus, reduce the complexity of the system and allow an unambiguous identification of the dominant NP properties.

By combining and varying the operating parameters, we were able to obtain catalysts with different physico-chemical properties (i.e., NP size, Pd oxidation state and Pd surface exposure). After the removal of the capping agent by gentle washing at 60 °C, the catalysts were tested in the liquid-phase hydrodeoxygenation (HDO) of benzaldehyde. Indeed, benzaldehyde's reduction is widely studied as model reaction for biomass valorization to fuels and many papers report the HDO of benzaldehyde to toluene under mild operating conditions using Pd-based catalysts. [24–26] The influence of the above-mentioned NP properties on the catalytic performance in the hydrogenation of benzaldehyde was carefully studied to identify the dominant parameters that determine the activity and stability of catalysts.

2. Results and Discussion

2.1. Catalyst Characterisation

In this study, the synthesis conditions associated with the sol-immobilization technique were varied to obtain catalysts with differences in their characteristics, specifically in their stabilizer/metal weight ratios, their solvents of synthesis and the rates of addition of their reducing agents. Poly (vinyl alcohol) (PVA) was used as stabilizer; the PVA/metal weight ratio was changed from 0.2 to 1.0, while two catalysts were prepared using either pure ethanol (EtOH) or a mixture of water and ethanol (1:1 *vol*/*vol*) as solvent instead of pure water used for the other synthesis. Finally, in order to decrease the reduction rate of the metal precursor, the synthesis was carried out by adding the reducing agent ($NaBH_4$) at different rates. Moreover, it should be pointed out that the reducing agent and metal precursor contain other elements such as Na, Cl and B, which can interfere with catalysis. In particular, Pd based catalysts are extensively influenced by chloride species. These species can facilitate particle sintering, while other impurities either distort or block the surface electronic interactions with the metal, leading to poor performance [27]. In addition, as highlighted in the Introduction, the capping agent could have a non-trivial effect on catalytic activity and selectivity. For all these reasons, extensive washing of the catalyst with warm water was performed after synthesis and before characterization.

The as-synthesized catalysts were labelled as w-Pd/$GNP_{x\text{-}y\text{-}z}$, where "x" represents the PVA/metal weight ratio, "y" represents the solvent of synthesis and "z" represents the rate of $NaBH_4$ addition; an additional "w" was placed in front of the catalysts that

underwent a washing step. For example, the w-Pd/$GNP_{0.5\text{-}H_2O\text{-}fast}$ sample represents the catalyst that was synthetized in pure water using a 0.5 PVA/metal weight ratio and a quick $NaBH_4$ addition, and that was fully washed of impurities and stabilizer at the end of the procedure.

The effectiveness of the washing steps on impurities and PVA removal was studied by XPS analysis. Considering the survey spectra (Figure S1) of all the unwashed samples, a relative atomic amount of Cl (derived from the metal precursor) of 0.09–0.12% was calculated, indicating that some chlorine species were present on the catalyst surface. On the contrary, no Cl species were detected on the washed samples. In the XPS survey analyses, no Na or B species were revealed, highlighting the efficiency of the washing procedure, which was performed on the basis of previous experience.

PVA removal was checked following the O/C ratio of the unwashed and washed samples. We noticed that the washed catalysts showed an O/C ratio that was lower than the respective as-synthesized catalysts (Table S1), and generally approaching that of bare GNP. For example, the bare support showed an O/C ratio of 0.056, while the unwashed Pd/$GNP_{0.5\text{-}H_2O\text{-}fast}$ sample had an O/C ratio of 0.084. After the washing of the catalysts, the O/C ratio decreased to 0.059, a value close to the one of the bare support. This behavior was observed for all the other samples as well. These results suggested that the washing procedure not only removed the impurities, but it was effective for the removal of the stabilizer as well. To confirm this analysis, the high-resolution spectra of the C 1s species were also evaluated (Table S1, Figure S2). Since the GNP is a highly graphitized support, the amount of surface hydroxyl/ether moieties (C–O), carbonyl groups (C=O) and carboxylic groups (O=C–O) is very low. The unwashed sample (for example, Pd/$GNP_{0.5\text{-}H_2O\text{-}fast}$) had a C–O concentration (35.2%) that was higher than that of the washed sample (26.1%) and the bare support (25.6%). Interestingly, all the washed samples presented a C–O concentration in the range of 23.9–26.8%, which was always lower than the C–O concentration in the corresponding unwashed catalysts. Therefore, these results provide further evidence of the nearly complete removal of PVA during the catalyst washing.

All the washed catalysts were characterized by ICP analysis in order to evaluate the experimental Pd loading (Table 1); values of 1.0 ± 0.1 wt% were obtained with all the samples, confirming that the washing step did not affect the anchoring of Pd nanoparticles to the surface of the support.

Table 1. Characterization results of the ICP, TEM and XPS analyses.

Catalyst	Metal Loading * (wt%)	Mean NPs Size § (nm)	$Pd_{exposure}$ ς (atomic %)	Pd(0) ς		$Pd(0)_{exposure}$ ° (%)
w-Pd/$GNP_{0.5\text{-}H_2O\text{-}fast}$	1.0 ± 0.1	3.6 ± 1.1	0.55	B.E. (eV) Atomic (%)	335.5 68	0.37
w-Pd/$GNP_{0.2\text{-}H_2O\text{-}fast}$	1.0 ± 0.1	4.6 ± 1.4	0.55	B.E. (eV) Atomic (%)	336.0 79	0.44
w-Pd/$GNP_{1.0\text{-}H_2O\text{-}fast}$	1.0 ± 0.1	4.4 ± 2.0	0.27	B.E. (eV) Atomic (%)	336.0 63	0.16
w-Pd/$GNP_{0.5\text{-}EtOH\text{-}fast}$	1.0 ± 0.1	5.7 ± 2.1	0.54	B.E. (eV) Atomic (%)	335.7 88	0.47
w-Pd/$GNP_{0.5\text{-}EtOH/H_2O\text{-}fast}$	1.0 ± 0.1	8.3 ± 3.9	0.37	B.E. (eV) Atomic (%)	335.9 93	0.34
w-Pd/$GNP_{0.5\text{-}H_2O\text{-}medium}$	1.1 ± 0.1	5.5 ± 2.1	0.37	B.E. (eV) Atomic (%)	335.7 99	0.36
w-Pd/$GNP_{0.5\text{-}H_2O\text{-}slow}$	1.0 ± 0.1	4.7 ± 1.5	0.45	B.E. (eV) Atomic (%)	336.1 99	0.45

* evaluated by ICP analysis, § evaluated by TEM analysis, ς evaluated by XPS analysis, ° product between $Pd_{exposure}$ and Pd(0).

TEM analyses (Figure 1) were used to evaluate the Pd NPs size and size distribution (Table 1, 3rd column, Figure S3). The synthesized catalysts showed a mean particle size range from 3.6 to 8.3 nm. The w-Pd/$GNP_{0.5\text{-}H_2O\text{-}fast}$ catalyst showed the smallest particle size, which was increased by reducing the $NaBH_4$ addition rate (medium or slow), probably due to the decreasing of the nucleation rate with respect to the growth rate. w-Pd/$GNP_{0.5\text{-}EtOH/H_2O\text{-}fast}$ showed the highest average diameter with a wide particle size distribution (Figure S3E). The particles were well dispersed on the support despite some agglomerations, particularly in the w-Pd/$GNP_{0.2\text{-}H_2O\text{-}fast}$ catalyst (Figure 1B). This catalyst was prepared with the lowest amount of stabilizer, and the NPs seemed to have agglomerated, possibly due to a reduced steric effect originating from the chemical bonding of the hydroxyl group of PVA to the metal.

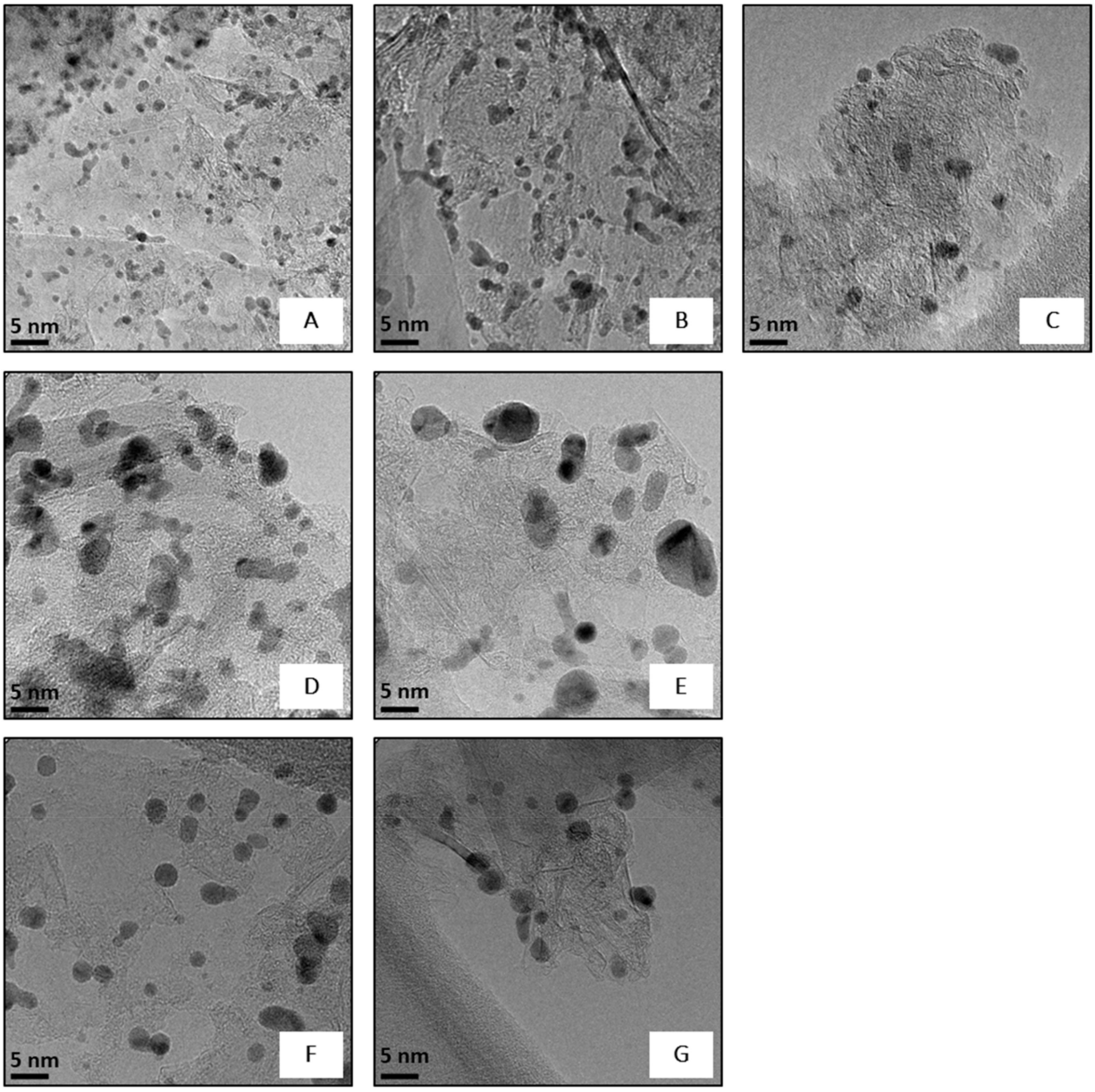

Figure 1. TEM images of the (**A**) w-Pd/$GNP_{0.5\text{-}H_2O\text{-}fast}$, (**B**) w-Pd/$GNP_{0.2\text{-}H_2O\text{-}fast}$, (**C**) w-Pd/$GNP_{1.0\text{-}H_2O\text{-}fast}$, (**D**) w-Pd/$GNP_{0.5\text{-}EtOH\text{-}fast}$, (**E**) w-Pd/$GNP_{0.5\text{-}EtOH/H_2O\text{-}fast}$, (**F**) w-Pd/$GNP_{0.5\text{-}H_2O\text{-}medium}$ and (**G**) w-Pd/$GNP_{0.5\text{-}H_2O\text{-}slow}$ catalyst.

The exposed Pd atomic % was evaluated from the survey spectra recorded during the XPS analyses, representing the atomic % of Pd detected on the catalyst surface. The Pd exposure on the GNP surface was in the range of 0.27–0.54%. The w-Pd/$GNP_{0.5\text{-}H_2O\text{-}fast}$ and w-Pd/$GNP_{0.2\text{-}H_2O\text{-}fast}$ catalysts showed very similar amounts of exposed Pd (0.55%), while unexpectedly, the catalyst synthesized using the highest capping agent amount (w-Pd/$GNP_{1.0\text{-}H_2O\text{-}fast}$) exhibited the lowest Pd exposure (0.27%) despite having a quite similar particle size. The relative amount of Pd(0) with respect to total exposed Pd was evaluated by deconvolving the Pd 3d region obtained from HR-XPS measurements (Figure 2).

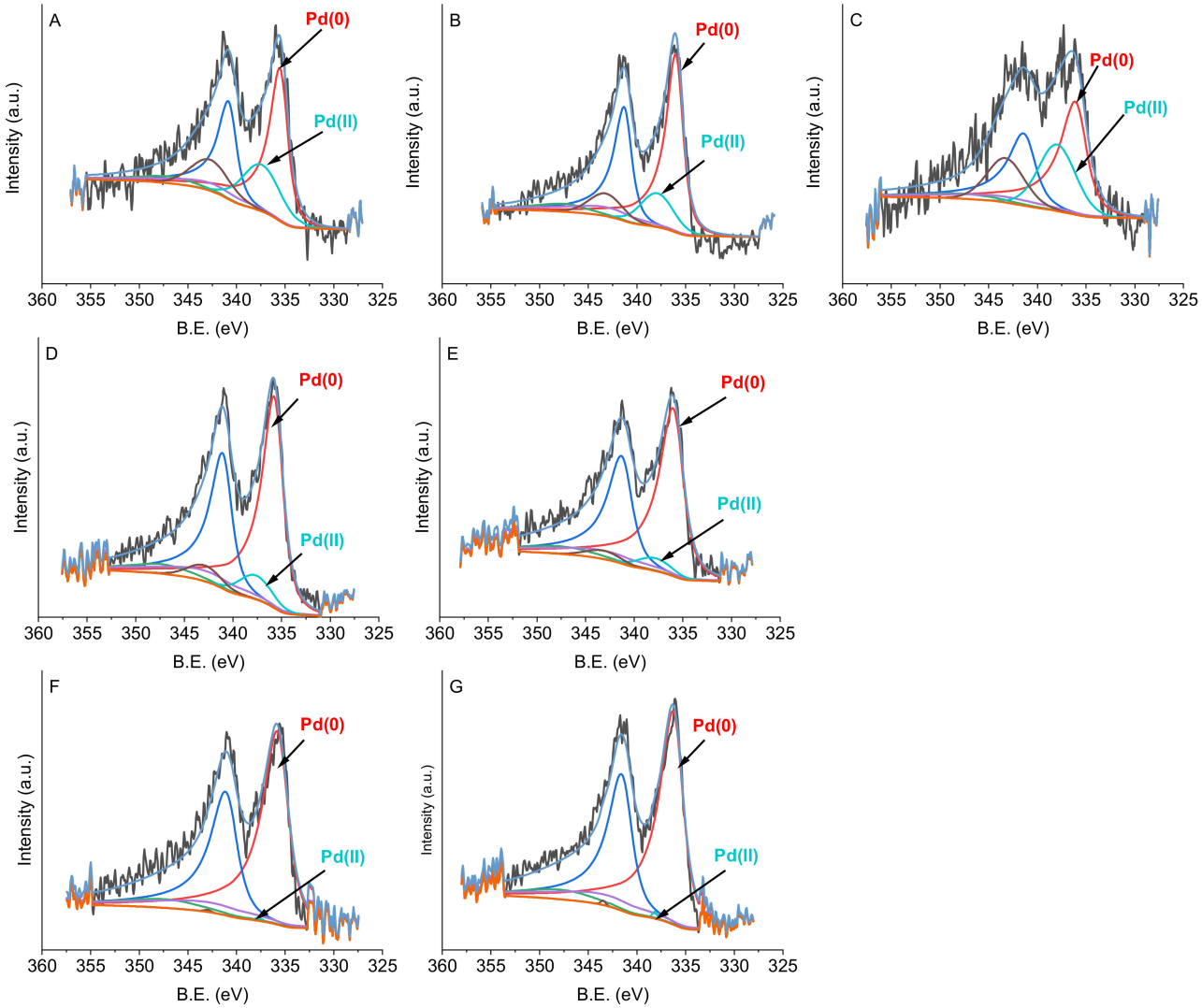

Figure 2. HR spectra of the Pd 3d region of (**A**) w-Pd/$GNP_{0.5\text{-}H_2O\text{-}fast}$, (**B**) w-Pd/$GNP_{0.2\text{-}H_2O\text{-}fast}$, (**C**) w-Pd/$GNP_{1.0\text{-}H_2O\text{-}fast}$, (**D**) w-Pd/$GNP_{0.5\text{-}EtOH\text{-}fast}$, (**E**) w-Pd/$GNP_{0.5\text{-}EtOH/H_2O\text{-}fast}$, (**F**) w-Pd/$GNP_{0.5\text{-}H_2O\text{-}medium}$ and (**G**) w-Pd/$GNP_{0.5\text{-}H_2O\text{-}slow}$ catalyst.

The relative Pd(0) amount was, in all samples, in the range of 63 to 99% (Table 1). When $NaBH_4$ is added to an aqueous solution, as the decomposition proceeds, the pH of the solution increases [28]. $NaBH_4$ is more stable at high pH, its decomposition slows down and its reducing power decreases. This implies that after 30 min, using water as solvent, the $NaBH_4$ decomposition is insufficient to completely reduce the metal precursor in the w-Pd/$GNP_{0.5\text{-}H_2O\text{-}fast}$ sample. By decreasing the addition rate of $NaBH_4$, the pH change is not as drastic and $NaBH_4$ decomposes faster, which, in turn, should increase the reduction rate of the metal precursor. This could explain why the catalysts prepared through the slow and medium addition of $NaBH_4$ (w-Pd/$GNP_{0.5\text{-}H_2O\text{-}medium}$ and w-Pd/$GNP_{0.5\text{-}H_2O\text{-}slow}$) showed

a complete reduction of the metal precursor (Pd(0) = 99%). In contrast, when $NaBH_4$ is added to a water/alcohol solution, its decomposition rate drastically increases, allowing a complete reduction in a short time [28]. This explains why the w-Pd/$GNP_{0.5\text{-EtOH-fast}}$ and w-Pd/$GNP_{0.5\text{-EtOH/}H_2O\text{-fast}}$ samples showed higher Pd(0) amounts (88% and 93%, respectively) than the w-Pd/$GNP_{0.5\text{-}H_2O\text{-fast}}$ catalyst (68%). When increasing the PVA/metal weight ratio from 0.2 to 1, the amount of Pd(0) decreased. This could be ascribed to the steric hindrance of PVA around the metal precursor, which limited the diffusion of the reducing agent to the metal precursor.

2.2. Catalytic Activity

The catalysts were tested in the hydrogenation of benzaldehyde under mild operating conditions (50 °C and 2 bar of H_2) in order to guarantee a kinetic regime. A general trend of the reaction is reported in Figure 3 for the w-Pd/$GNP_{0.5\text{-}H_2O\text{-fast}}$ catalyst. The hydrogenation reaction of benzaldehyde followed a typical consecutive reaction pathway, with an initial hydrogenation step to benzyl alcohol followed by hydrodeoxygenation to form toluene.

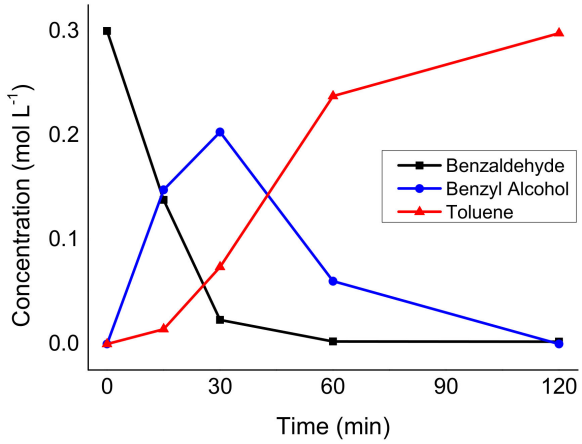

Figure 3. Reaction profile using the Pd/$GNP_{0.5\text{-}H_2O\text{-fast}}$ catalyst. Reaction conditions: 50 °C, 2 bar of H_2, substrate/metal ratio of 1000:1 mol/mol.

The catalytic activity was evaluated using Equation (3), and it is reported in Table 2. As already mentioned, the stabilizer can have a great impact on the performance of metal NPs due to the hindered contact of the substrate on the active site and its chemical nature [7,12,13]. Therefore, the removal of PVA from the catalyst surface could increase the catalyst activity. The impact of residual PVA was first evaluated by comparing the performances of Pd/$GNP_{0.5\text{-}H_2O\text{-fast}}$ and the corresponding washed sample (w-Pd/$GNP_{0.5\text{-}H_2O\text{-fast}}$). An expected increase in initial activity was observed by washing off the PVA (from 0.48 to 0.59 s^{-1}). By removing the stabilizer, the metal surface was more accessible for substrate adsorption and subsequent conversion, thus increasing the reaction rate. A general trend was obtained overall when considering all other unwashed and washed catalysts: post-synthesis washing increases the catalyst activity. The washed samples showed an initial activity in the range of 0.34–0.79 s^{-1} and, after 15 min of reaction, the selectivity towards benzyl alcohol was close to 90% in all cases. After 2 h of reaction, all catalysts had fully converted benzaldehyde into toluene (reaction profiles are reported in Figure S4).

Table 2. Catalytic results of the various synthesized catalysts.

Sample	Initial Activity * (s^{-1})	Conversion * (%)	$Selectivity_{benzyl\ alcohol}$ * (%)	$Selectivity_{toluene}$ * (%)
$Pd/GNP_{0.5\text{-}H_2O\text{-}fast}$	0.48	40	88	12
$w\text{-}Pd/GNP_{0.5\text{-}H_2O\text{-}fast}$	0.59	54	91	9
$w\text{-}Pd/GNP_{0.2\text{-}H_2O\text{-}fast}$	0.66	60	94	6
$w\text{-}Pd/GNP_{1.0\text{-}H_2O\text{-}fast}$	0.34	31	91	9
$w\text{-}Pd/GNP_{0.5\text{-}EtOH\text{-}fast}$	0.79	72	91	9
$w\text{-}Pd/GNP_{0.5\text{-}EtOH/H_2O\text{-}fast}$	0.54	49	95	5
$w\text{-}Pd/GNP_{0.5\text{-}H_2O\text{-}medium}$	0.60	54	94	6
$w\text{-}Pd/GNP_{0.5\text{-}H_2O\text{-}slow}$	0.76	70	94	6

* calculated after 15 min of reaction. Reaction conditions: 50 °C, 2 bar of H_2, substrate/metal ratio of 1000:1 mol/mol.

2.3. Activity/Catalyst Properties Correlation

Characterization and kinetic results were brought together in order to identify the dominant catalyst features that determined the hydrogenation activity of benzaldehyde. Considering the NPs' size and initial activity, no particular trend was observed (Figure S5). In fact, catalysts that exhibited a similar average diameter often showed different initial activity. For example, the $w\text{-}Pd/GNP_{0.2\text{-}H_2O\text{-}fast}$, $w\text{-}Pd/GNP_{1.0\text{-}H_2O\text{-}fast}$ and $w\text{-}Pd/GNP_{0.5\text{-}H_2O\text{-}slow}$ catalysts showed an activity of 0.66, 0.34, 0.76 s^{-1}, respectively, despite having similar Pd NP sizes, i.e., 4.4, 4.6 and 4.7 nm, respectively (Table 1). Therefore, the analysis was extended to other catalyst surface properties.

In this regard, the amount of exposed Pd derived from the XPS survey spectra was considered next. Furthermore, in this case, no regular trend was obtained, since catalysts with the same Pd exposure gave different initial activities (Figure S6A) even if it was observed that increased Pd exposure led to increased activity.

We thus turned our attention to the relative Pd(0) amount, for which the initial activity seemed to increase with the metallic Pd percentage, although some deviations from this trend could be observed (Figure S6B). It is well known that hydrogenation/hydrogenolysis reactions mainly occur on metallic Pd thanks to easier hydrogen dissociation towards surface H species, which reduce carbonyl groups and C–C double bonds [29,30]. Considering the emerging trends between the initial activity, Pd exposure and relative Pd(0) amount, we then looked at the exposed Pd(0) concentration (referred to as $Pd(0)_{exposed}$) that could be calculated by multiplying the $Pd_{exposure}$ and the relative Pd(0) amount (Equation (1)).

$$Pd(0)_{exposed}(\%) = \frac{Pd_{exposed}}{100} \cdot Pd(0) \quad (1)$$

This value represents the amount of Pd(0) exposed at the surface relative to the total available catalyst surface. Table 1 reports all the calculated values. By plotting the initial activity vs. the amount of exposed Pd(0), we successfully obtained a linear trend (Figure 4), implying that the reaction rate of the hydrogenation of benzaldehyde is mainly ruled by the concentration of exposed Pd(0). The latter can be tuned by adapting the synthetic methodology used.

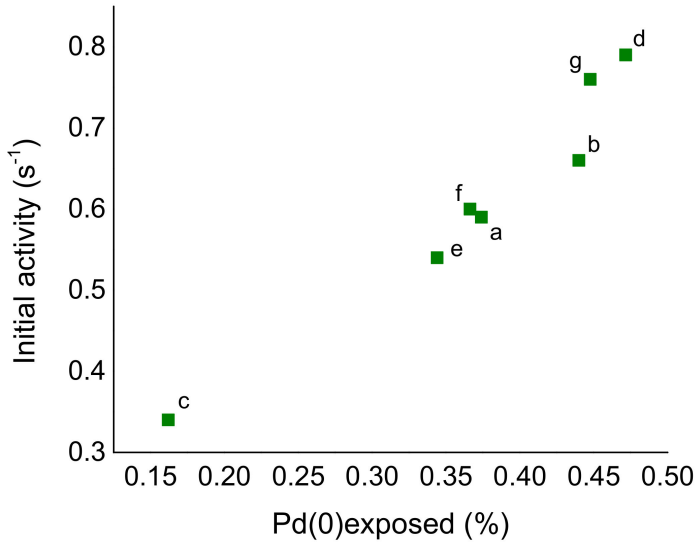

Figure 4. Influence of the exposed Pd(0) on the initial activity of the different catalysts: (**a**) Pd/GNP$_{0.5\text{-}H_2O\text{-}fast}$, (**b**) Pd/GNP$_{0.2\text{-}H_2O\text{-}fast}$, (**c**) Pd/GNP$_{1.0\text{-}H_2O\text{-}fast}$, (**d**) Pd/GNP$_{0.5\text{-}EtOH\text{-}fast}$, (**e**) Pd/GNP$_{0.5\text{-}EtOH/H_2O\text{-}fast}$, (**f**) Pd/GNP$_{0.5\text{-}H_2O\text{-}medium}$ and (**g**) Pd/GNP$_{0.5\text{-}H_2O\text{-}slow}$.

Recycling tests were also performed on w-Pd/GNP$_{0.5\text{-}H_2O\text{-}fast}$ to study the catalyst stability (Figure 5). After 15 min, the conversion and product selectivity remained stable after at least four cycles. The spent catalyst recovered at the end of the fourth run was characterized to detect any significant changes to the surface properties. XPS analysis of the used catalyst revealed a lower Pd exposure than the one present in the fresh sample (0.43% versus 0.55%, respectively, Table 3); however, this was counteracted by an increase in the relative amount of metallic Pd (from 80 to 87%). This increase was consistent with the reducing environment employed for the reaction, which was able to partially reduce Pd(II) to Pd(0) [31]. Overall, the fresh and used catalysts exhibited the same amount of exposed Pd(0) on the catalyst surface, which explains their similar initial activities, and further confirms the correlation between Pd(0)$_{exposed}$ and activity (Table 3).

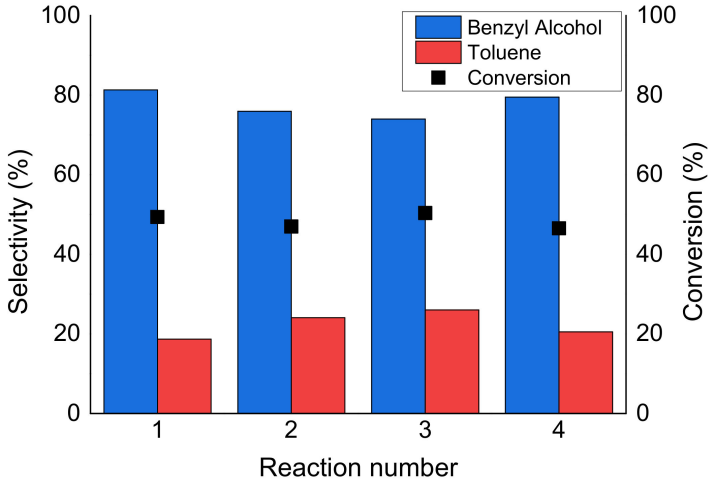

Figure 5. Results of the recycling tests with the Pd/GNP$_{0.5\text{-}H_2O\text{-}fast}$ catalyst. Conversion (black squares) and products selectivity (bars) were evaluated after 15 min of reaction.

Table 3. Comparison of the XPS results of the fresh and used catalyst.

Catalyst	$Pd_{exposure}$ (Atomic %)	Pd(0) (Atomic %)	$Pd(0)_{exposure}$ (%)
w-Pd/$GNP_{0.5\text{-}H_2O\text{-}fast}$ fresh	0.55	68	0.37
w-Pd/$GNP_{0.5\text{-}H_2O\text{-}fast}$ used	0.43	87	0.37

3. Materials and Methods

Poly(vinyl alcohol) (PVA), benzaldehyde, *p*-xylene, $Na_2PdCl_4{\cdot}4H_2O$, $NaBH_4$ and H_2SO_4 were purchased from Merk (Darmstadt, Germany). Grade-C Graphene Nanoplatelets (GNP-500) were purchased from XG-Science (Lansing, MI, USA).

3.1. Catalyst Syntheses

The 1%Pd/GNP catalysts were prepared using the sol-immobilization method and, by varying the synthesis parameters, catalysts of different Pd NP sizes were obtained [23].

Generally, 100 mL of solvent (milliQ-grade water or EtOH) were degassed under nitrogen flow for 1 h in a round-bottom flask to eliminate the dissolved oxygen (the nitrogen flow was kept constant throughout the whole synthesis). Then, the degassed solvent was heated to 30 °C; 2 mL of Pd precursor (Na_2PdCl_4, 5 mg/mL) was added under vigorous stirring. Subsequently, the stabilizer (PVA, 1 wt%) was added in the desired amount, while a fresh solution of $NaBH_4$ (0.15 M) was prepared and 5 mL was added to the Pd precursor solution at different rates (as reported in Table 4). The colloidal suspension was then maintained under vigorous stirring for 30 min. A quantity of 0.99 g of the GNP support was then added to the Pd suspension and 3 drops of concentrated H_2SO_4 were introduced to enhance the Pd immobilization on the support (pH 2). The immobilization step lasted 1 h under constant nitrogen flow and vigorous stirring. Finally, the catalyst was filtered and washed until neutral pH was reached. In Table 4, the list of the synthesized catalysts and the operating conditions used for each synthesis are reported.

Table 4. Operating parameters used for the catalysts' syntheses.

Catalysts	PVA/Metal (wt%/wt%)	Solvent	$NaBH_4$ Addition
w-Pd/$GNP_{0.5\text{-}H_2O\text{-}fast}$	0.5	H_2O	Instantaneous
w-Pd/$GNP_{0.2\text{-}H_2O\text{-}fast}$	0.2	H_2O	Instantaneous
w-Pd/$GNP_{1.0\text{-}H_2O\text{-}fast}$	1.0	H_2O	Instantaneous
w-Pd/$GNP_{0.5\text{-}EtOH\text{-}fast}$	0.5	EtOH	Instantaneous
w-Pd/$GNP_{0.5\text{-}EtOH/H_2O\text{-}fast}$	0.5	EtOH/H_2O (1:1 *vol*/*vol*)	Instantaneous
w-Pd/$GNP_{0.5\text{-}H_2O\text{-}medium}$	0.5	H_2O	Over 2 min
w-Pd/$GNP_{0.5\text{-}H_2O\text{-}slow}$	0.5	H_2O	Over 4 min

3.2. Catalyst Washing

Removal of the impurities (Na, Cl, S, B) and PVA was performed by suspending 0.5 g of catalyst in 50 mL of milliQ-grade water three times at 60 °C for 30 min under vigorous stirring. The efficiency of the washing process was checked by recording X-ray photoelectron spectroscopy (XPS) spectra.

The washed samples were labelled by adding the prefix "w" to the respective catalyst labels.

3.3. Catalysts Characterization

Inductively coupled plasma (ICP) analysis was performed to evaluate the nominal Pd loading of the catalysts. Before the analysis, 0.07 g of catalyst was added to 4.0 mL of

HNO_3 and 1.0 mL of H_2O_2. The mixture was then placed in a microwave setup with a heating ramp from 25 °C to 200 °C at 10 °C min^{-1}. The maximum temperature was kept constant for 20 min. The digested samples were then cooled at room temperature and the solution was recovered using milliQ-grade water. The samples were diluted to obtain a final calculated Pd concentration of 2 ppm. Sample digestion and ICP were performed 2 times to verify the reliability of the protocol.

Transmission electron microscopy (TEM) analyses were carried out on a FEI Tecnai F20 microscope in order to evaluate the Pd NPs' sizes. The instrument was equipped with a Field Emission Gun (FEG) and operated at an accelerating voltage of 200 kV. Samples were prepared by sonication of the sample in isopropanol followed by deposition on 300-mesh copper grids coated with lacey carbon film. Histograms of the particle size distribution (PSD) were obtained by counting at least 500 particles. The mean particle diameter (dm) was calculated using the formula $dm = \sum d_i n_i / \sum n_i$ where n_i is the number of particles of diameter d_i.

X-ray photoelectron spectroscopy (XPS) was performed on bare support and washed samples. The survey and the high-resolution spectra (HR) of C1s and Pd 3d regions were acquired using an M-probe apparatus. The spectra were recorded by using an Al Kα X-ray line.

3.4. Catalytic Reactions

Benzaldehyde hydrogenation reactions were performed in a 100 mL stainless steel autoclave under mild conditions (50 °C, 2 bar of H_2) using *p*-xylene as a solvent. In a typical experiment, 10 mL of a 0.3 M solution of benzaldehyde in *p*-xylene and an appropriate amount of catalyst (substrate-to-metal molar ratio of 1000:1) were placed into a glass inlet inside the autoclave along with a magnetic stirrer. The system was first flushed several times with N_2 to remove any residual oxygen in the atmosphere, and then pressurized with H_2 to 2 bar. The reaction was then heated at 50 °C and the solution stirred at a constant stirring rate of 1000 rpm. Samplings were carried out by stopping the stirring and quenching of the reaction in an ice bath. Product identification was carried out with a GC-MS (Thermo Scientific, USA, ISQ QD equipped with an Agilent, USA, VF-5 ms column), while product quantification was carried by GC-FID analysis (Thermo Scientific TRACE 1300 equipped with an Agilent, USA, HP-5 column). Benzaldehyde conversion was evaluated using Equation (2)

$$Conversion\ (\%) = \frac{n_{t=0} - n_t}{n_{t=0}} \quad (2)$$

where $n_{t=0}$ are the moles of benzaldehyde introduced in the reactor, while n_t are the remaining moles after a reaction time t. Product selectivities were also calculated.

The catalyst initial activity was calculated after 15 min of reaction using Equation (3)

$$Initial\ acitivity\ \left(s^{-1}\right) = \frac{n_{t=0} - n_{t=15\ min}}{mol_{Pd} \cdot reaction\ time\ (s)} \quad (3)$$

where mol_{Pd} are the moles of Pd introduced in the reactor, and the reaction time is 15 min (900 s).

3.5. Recycling Tests

Recycling tests were performed to study the catalyst stability and its chemical properties after reusing it 4 times. Each reaction was performed for 15 min followed by catalyst recovery, washing and drying at room temperature before reuse.

4. Conclusions

Hydrodeoxygenation reactions are vital in the upgrading of biomass-derived compounds to added-value chemicals or bio-fuels. Heterogeneous catalysts are widely employed for these reactions, and studies on the relation between catalyst performance and

its properties are fundamental to improve the design of catalysts. In this work, Pd NPs supported on a highly graphitized support (graphene nanoplates) were prepared by means of the sol-immobilization technique, with the stabilizer amount, solvent and reducing-agent addition rate being varied. The variation of the synthesis parameters made it possible to obtain catalysts with different Pd particle sizes and different surface properties. The catalytic performance was evaluated using the hydrogenation of benzaldehyde as a model reaction. All the catalysts showed full conversion to toluene after 2 h of reaction, but generally exhibited a different initial activity evaluated after 15 min of reaction. While the activity and Pd particle size seemed uncorrelated, we found a linear correlation between the initial activity and the amount of exposed Pd(0), calculated as the product of the total exposed Pd and the Pd(0) fraction. Catalyst recycling tests showed no loss of activity and selectivity after at least four cycles. Characterization of the used catalyst after the fourth recycle test indicated a higher relative Pd(0) amount and a lower Pd exposure compared to the fresh catalyst, leading to a comparable Pd(0) exposure overall. This confirmed the direct correlation between the initial activity and the $Pd(0)_{exposed}$ fraction (representing the Pd(0) exposure) in the HDO reaction. This finding could help in the design of HDO catalysts.

Supplementary Materials: The following are available online at https://www.mdpi.com/article/10.3390/catal12030251/s1, Figure S1: Survey spectra, Figure S2: C1s region, Figure S3: Particle size distribution obtained from TEM analyses, Figure S4: Reaction profile, Figure S5: Influence of NPs size on the initial activity of the different catalysts, Figure S6: Influence of the A) Pd exposure and B) Pd(0) amount on the activity of the different catalysts, Table S1: Results of the XPS analysis.

Author Contributions: Conceptualization, S.C. (Sofia Capelli) and S.C. (Stefano Cattaneo); methodology, S.C. (Sofia Capelli) and S.C. (Stefano Cattaneo); validation, S.C. (Sofia Capelli), S.C. (Stefano Cattaneo) and M.S.; formal analysis, S.C. (Sofia Capelli) and S.C. (Stefano Cattaneo); investigation, S.C. (Sofia Capelli) and S.C. (Stefano Cattaneo); resources, L.P., B.D.V. and A.C.; writing—original draft preparation, S.C. (Sofia Capelli); writing—review and editing, L.P. and A.V.; supervision, L.P.; project administration, B.D.V. and A.C. All authors have read and agreed to the published version of the manuscript.

Funding: This research received financial support from TotalEnergies "Consortium on Metal Nanocatalysis" project.

Acknowledgments: The authors acknowledge the TotalEnergies "Consortium on Metal Nanocatalysis" project for the funding of this project.

Conflicts of Interest: The authors declare no conflict of interest.

References

1. Personick, M.L.; Montemore, M.M.; Kaxiras, E.; Madix, R.J.; Biener, J.; Friend, C.M. Catalyst Design for Enhanced Sustainability through Fundamental Surface Chemistry. *Philos. Trans. R. Soc. A Math. Phys. Eng. Sci.* **2016**, *374*, 20150077. [CrossRef] [PubMed]
2. Wang, X.; Li, G.; Ozkan, U.S. Hydrogenation of Hexanal over Sulfided Ni-Mo/γ-Al_2O_3 Catalysts. *J. Mol. Catal. A Chem.* **2004**, *217*, 219–229. [CrossRef]
3. Fu, J.; Lu, X.; Savage, P.E. Hydrothermal Decarboxylation and Hydrogenation of Fatty Acids over Pt/C. *ChemSusChem* **2011**, *4*, 481–486. [CrossRef] [PubMed]
4. Villa, A.; Wang, D.; Veith, G.M.; Vindigni, F.; Prati, L. Sol Immobilization Technique: A Delicate Balance between Activity, Selectivity and Stability of Gold Catalysts. *Catal. Sci. Technol.* **2013**, *3*, 3036–3041. [CrossRef]
5. Sanchez, F.; Motta, D.; Bocelli, L.; Albonetti, S.; Roldan, A.; Hammond, C.; Villa, A.; Dimitratos, N. Investigation of the Catalytic Performance of Pd/CNFs for Hydrogen Evolution from Additive-Free Formic Acid Decomposition. *C* **2018**, *4*, 26. [CrossRef]
6. Sanchez, F.; Motta, D.; Roldan, A.; Hammond, C.; Villa, A.; Dimitratos, N. Hydrogen Generation from Additive-Free Formic Acid Decomposition Under Mild Conditions by Pd/C: Experimental and DFT Studies. *Top. Catal.* **2018**, *61*, 254–266. [CrossRef]
7. Alijani, S.; Capelli, S.; Cattaneo, S.; Schiavoni, M.; Evangelisti, C.; Mohammed, K.M.H.; Wells, P.P.; Tessore, F.; Villa, A. Capping Agent Effect on Pd-Supported Nanoparticles in the Hydrogenation of Furfural. *Catalysts* **2019**, *10*, 11. [CrossRef]
8. Baygazieva, E.K.; Yesmurzayeva, N.N.; Tatykhanova, G.S.; Mun, G.A.; Khutoryanskiy, V.V.; Kudaibergenov, S.E. Polymer Protected Gold Nanoparticles: Synthesis, Characterization and Application in Catalysis. *J. Biol. Chem.* **2014**, *7*, 14–23. [CrossRef]
9. Raveendran, P.; Fu, J.; Wallen, S.L. Completely "Green" Synthesis and Stabilization of Metal Nanoparticles. *J. Am. Chem. Soc.* **2003**, *125*, 13940–13941. [CrossRef]

10. Crooks, R.M.; Zhao, M.; Sun, L.; Chechik, V.; Yeung, L.K. Dendrimer-Encapsulated Metal Nanoparticles: Synthesis, Characterization, and Applications to Catalysis. *Acc. Chem. Res.* **2001**, *34*, 181–190. [CrossRef]
11. Smith, D.K.; Korgel, B.A. The Importance of the CTAB Surfactant on the Colloidal Seed-Mediated Synthesis of Gold Nanorods. *Langmuir* **2008**, *24*, 644–649. [CrossRef] [PubMed]
12. Li, D.; Wang, C.; Tripkovic, D.; Sun, S.; Markovic, N.M.; Stamenkovic, V.R. Surfactant Removal for Colloidal Nanoparticles from Solution Synthesis: The Effect on Catalytic Performance. *ACS Catal.* **2012**, *2*, 1358–1362. [CrossRef]
13. Niu, Z.; Li, Y. Removal and Utilization of Capping Agents in Nanocatalysis. *Chem. Mater.* **2014**, *26*, 72–83. [CrossRef]
14. Ajitha, B.; Kumar Reddy, Y.A.; Reddy, P.S.; Jeon, H.-J.; Ahn, C.W. Role of Capping Agents in Controlling Silver Nanoparticles Size, Antibacterial Activity and Potential Application as Optical Hydrogen Peroxide Sensor. *RSC Adv.* **2016**, *6*, 36171–36179. [CrossRef]
15. Phan, C.M.; Nguyen, H.M. Role of Capping Agent in Wet Synthesis of Nanoparticles. *J. Phys. Chem. A* **2017**, *121*, 3213–3219. [CrossRef]
16. Neri, G.; Musolino, M.G.; Milone, C.; Pietropaolo, D.; Galvagno, S. Particle Size Effect in the Catalytic Hydrogenation of 2,4-Dinitrotoluene over Pd/C Catalysts. *Appl. Catal. A Gen.* **2001**, *208*, 307–316. [CrossRef]
17. Johnson, J.A.; Makis, J.J.; Marvin, K.A.; Rodenbusch, S.E.; Stevenson, K.J. Size-Dependent Hydrogenation of p-Nitrophenol with Pd Nanoparticles Synthesized with Poly(Amido)Amine Dendrimer Templates. *J. Phys. Chem. C* **2013**, *117*, 22644–22651. [CrossRef]
18. Gao, D.; Zhou, H.; Wang, J.; Miao, S.; Yang, F.; Wang, G.; Wang, J.; Bao, X. Size-Dependent Electrocatalytic Reduction of CO_2 over Pd Nanoparticles. *J. Am. Chem. Soc.* **2015**, *137*, 4288–4291. [CrossRef]
19. Wilson, O.M.; Knecht, M.R.; Garcia-Martinez, J.C.; Crooks, R.M. Effect of Pd Nanoparticle Size on the Catalytic Hydrogenation of Allyl Alcohol. *J. Am. Chem. Soc.* **2006**, *128*, 4510–4511. [CrossRef]
20. Zorn, K.; Giorgio, S.; Halwax, E.; Henry, C.R.; Grönbeck, H.; Rupprechter, G. CO Oxidation on Technological Pd-Al_2O_3 Catalysts: Oxidation State and Activity. *J. Phys. Chem. C* **2011**, *115*, 1103–1111. [CrossRef]
21. Xiong, H.; Wiebenga, M.H.; Carrillo, C.; Gaudet, J.R.; Pham, H.N.; Kunwar, D.; Oh, S.H.; Qi, G.; Kim, C.H.; Datye, A.K. Design Considerations for Low-Temperature Hydrocarbon Oxidation Reactions on Pd Based Catalysts. *Appl. Catal. B Environ.* **2018**, *236*, 436–444. [CrossRef]
22. Lv, Q.; Meng, Q.; Liu, W.; Sun, N.; Jiang, K.; Ma, L.; Peng, Z.; Cai, W.; Liu, C.; Ge, J.; et al. Pd–PdO Interface as Active Site for HCOOH Selective Dehydrogenation at Ambient Condition. *J. Phys. Chem. C* **2018**, *122*, 2081–2088. [CrossRef]
23. Capelli, S.; Motta, D.; Evangelisti, C.; Dimitratos, N.; Prati, L.; Pirola, C.; Villa, A. Effect of Carbon Support, Capping Agent Amount, and Pd NPs Size for Bio-Adipic Acid Production from Muconic Acid and Sodium Muconate. *Nanomaterials* **2020**, *10*, 505. [CrossRef] [PubMed]
24. Guo, X.-F.; Jang, D.-Y.; Jang, H.-G.; Kim, G.-J. Hydrogenation and Dehydrogenation Reactions Catalyzed by CNTs Supported Palladium Catalysts. *Catal. Today* **2012**, *186*, 109–114. [CrossRef]
25. Menegazzo, F.; Canton, P.; Pinna, F.; Pernicone, N. Bimetallic Pd–Au Catalysts for Benzaldehyde Hydrogenation: Effects of Preparation and of Sulfur Poisoning. *Catal. Commun.* **2008**, *9*, 2353–2356. [CrossRef]
26. Divakar, D.; Manikandan, D.; Kalidoss, G.; Sivakumar, T. Hydrogenation of Benzaldehyde over Palladium Intercalated Bentonite Catalysts: Kinetic Studies. *Catal. Lett.* **2008**, *125*, 277. [CrossRef]
27. Simone, D.O.; Kennelly, T.; Brungard, N.L.; Farrauto, R.J. Reversible Poisoning of Palladium Catalysts for Methane Oxidation. *Appl. Catal.* **1991**, *70*, 87–100. [CrossRef]
28. Fernandes, V.R.; Pinto, A.M.F.R.; Rangel, C.M. Hydrogen Production from Sodium Borohydride in Methanol–Water Mixtures. *Int. J. Hydrogen Energy* **2010**, *35*, 9862–9868. [CrossRef]
29. López-Corral, I.; Germán, E.; Juan, A.; Volpe, M.A.; Brizuela, G.P. DFT Study of Hydrogen Adsorption on Palladium Decorated Graphene. *J. Phys. Chem. C* **2011**, *115*, 4315–4323. [CrossRef]
30. Cabria, I.; López, M.J.; Fraile, S.; Alonso, J.A. Adsorption and Dissociation of Molecular Hydrogen on Palladium Clusters Supported on Graphene. *J. Phys. Chem. C* **2012**, *116*, 21179–21189. [CrossRef]
31. Capelli, S.; Motta, D.; Evangelisti, C.; Dimitratos, N.; Prati, L.; Pirola, C.; Villa, A. Bio Adipic Acid Production from Sodium Muconate and Muconic Acid: A Comparison of Two Systems. *ChemCatChem* **2019**, *11*, 3075–3084. [CrossRef]